Inorg. Chem. **1986**, *25*, 1239–1242

Contribution No. 3899 from the Central Research & Development Department,
E. I. du Pont de Nemours & Company, Experimental Station, Wilmington, Delaware 19898

Synthesis and ^{183}W NMR Characterization of Vanadium-Substituted Polyoxometalates Based on B-Type $PW_9O_{34}^{9-}$ Precursors

Peter J. Domaille* and George Watunya

Received October 14, 1985

The syntheses and characterizations of the di- and trivanadophosphotungstates 1,4-$PV_2W_{10}O_{40}^{5-}$ and 1,4,9-$PV_3W_9O_{40}^{6-}$ are described. These compounds contain adjacent vanadium-centered octahedra of oxygen atoms with a common edge, in contrast to previously reported compounds that share a common corner oxygen vertex. Edge-shared vanadium atoms offer the attractive possibility for support of organometallic moieties. Both compounds are characterized by 1-D and 2-D ^{183}W NMR, 1-D ^{31}P and ^{51}V NMR, and IR spectroscopy.

Introduction

We recently published[1] a paper detailing the synthesis and 2-D ^{183}W NMR characterization of specific positional isomers[2] of di- and trisubstituted vanado*phospho*tungstates. A prior report by Mossoba and co-workers,[3] in connection with particular isomers of the Keggin structure, dealt with the corresponding vanado*silico*tungstate family. Recently, Finke et al.[4] also disclosed a related trivanado-substituted silicotungstate based on the Baker–Figgis β-isomer.[5] In all the above compounds vanadium atoms occupy adjacent sites with a common corner vertex oxygen atom. These structures were anticipated for the silicotungstates since the syntheses used the well-characterized[6] precursors A,α-$SiW_9O_{34}^{10-}$ (Mossoba) and A,β-$SiW_9O_{34}^{10-}$ (Finke), each possessing the required tungsten vacancies.

On the other hand, the structure of reactant $PW_9O_{34}^{9-}$ used in our syntheses is more uncertain. Originally, the compound was assigned[7] a B,β structure, but as Pope[8] remarks, the existence of both α- and β-isomers (distinguished polarographically) argues against this B-type geometry. A recent partial crystal structure,[9] on a compound we presume to contain the same anion, is unable to provide definitive evidence. Our products[1] suggested an A-type precursor, and more recent[10] reaction chemistry was also rationalized on the basis of an A-type structure. Consistent with this formulation, solid-state ^{31}P NMR shows[10] the compound goes through a solid-state rearrangement, converting from A type to the B form, upon moderate heating.

Herein, we extend these findings to devise synthetic procedures for new di- and trisubstituted vanadophosphotungstates in which the vanadium atoms share common *edge* pairs of oxygen atoms. Products with this structural feature will provide sterically accessible basic sites for κ^3-support of organometallic groups.[11]

Our compounds are characterized by elemental analysis and by conventional IR and NMR spectroscopy. Structural information is obtained from 1- and 2-D ^{183}W{^{51}V} NMR by using established principles[1] for mapping the tungsten–vanadium atom framework.

Experimental Section

^{31}P, ^{51}V, and ^{183}W NMR spectra were obtained with a Nicolet NT-360WB spectrometer by using previously described procedures.[1] Spectra

---

(1) Domaille, P. J. *J. Am. Chem. Soc.* **1984**, *106*, 7677–7687.

(2) (a) Pope, M. T.; Scully, T. F. *Inorg. Chem.* **1975**, *14*, 953–954. (b) Pope, M. T.; O'Donnell, S. E.; Prados, R. A. *J. Chem. Soc., Chem. Commun.* **1976**, 85–94.

(3) (a) Mossoba, M. M.; O'Connor, C. J.; Pope, M. T.; Sinn, E.; Hervé, G.; Tèzé, A. *J. Am. Chem. Soc.* **1980**, *102*, 6864–6866. (b) We have reported the isolation of a single positional isomer of 1,5-$PTi_2W_{10}O_{40}^{7-}$, but the reason for the exclusive generation of this product was not apparent: Domaille, P. J.; Knoth, W. H. *Inorg. Chem.* **1983**, *22*, 818–822.

(4) Finke, R. G.; Rapko, B.; Saxton, R. J.; Domaille, P. J., submitted for publication in *Inorg. Chem.*

(5) (a) Baker, L. C. W.; Figgis, J. S. *J. Am. Chem. Soc.* **1970**, *92*, 3794–3797. (b) See: Pope, M. T. "Heteropoly and Isopolymetalates"; Springer-Verlag: New York, 1983; p 27.

(6) The better characterized compound is the β-form, which is supported by a crystal structure: Robert, F.; Tèzé, A. *Acta Crystallogr., Sect. B: Struct. Crystallogr. Cryst. Chem.* 1981, *B37*, 318–322. Synthetic details and polarographic data for the α- and β-species are reported in: Hervé, G.; Tèzé, A. *Inorg. Chem.* **1977**, *16*, 2115–2117.

(7) Massart, R.; Contant, R.; Fruchart, J. M.; Ciabrini, J. P.; Fournier, M. *Inorg. Chem.* **1977**, *16*, 2916–2921.

(8) Pope, M. T. Reference 5b, p 68.

(9) Fuchs, J.; Palm, R. *Z. Naturforsch., B: Anorg. Chem., Org. Chem.* **1984**, *39B*, 757–762.

(10) (a) Knoth, W. H.; Domaille, P. J.; Farlee, R. D. Organometallics **1985**, *4*, 62–68. (b) Knoth, W. H.; Domaille, P. J.; Harlow, R. L., submitted for publication in *Inorg. Chem.*

(11) Organometallic species have been reported supported on disubstituted hexametalates (Besecker, C. J.; Day, V. W.; Klemperer, W. G.; Thompson, M. R. *Inorg. Chem.* **1985**, *24*, 44–50 and references therein) and on A-type trisubstituted Keggin anions (Finke, R. G.; Droege, M. W. *J. Am. Chem. Soc.* **1984**, *106*, 7274–7277. Finke, R. G.; Rapko, B.; Domaille, P. J., submitted for publication in *Organometallics*). Professor Finke has pointed out that B-type trisubstituted anions would be preferable because of the greater accessibility of the edge bridging oxygens. This structural feature is present in $V_3W_3O_{19}^{5-}$ and $P_2V_3W_{15}O_{62}^{9-}$ but has not hitherto been reported in $PV_3W_9O_{40}^{6-}$ (Keggin) structures. Vanadium substitution also appears preferable to that of niobium in producing basic sites of attachment because of the tendency of the latter produce dimers.

(12) The mathematics of this problem and some usual NMR configurations are described in: Homer, J. *J. Magn. Reson.* **1984**, *57*, 171–177. The result of interest for our case is that ^{31}P chemical shifts in a vertical B_0 configuration are related to those in a horizontal B_0 mode by $\delta_{\mathrm{vert}}(^{31}\mathrm{P}) = \delta_{\mathrm{horiz}}(^{31}\mathrm{P}) + 0.70$ ppm. The 0.70 ppm factor is experimentally measured as the difference between the chemical shift of $Li_4[PVW_{11}O_{40}]$ relative to 85% H_3PO_4 at 30 °C on an XL-100 (horizontal B_0) and our NT-360 (vertical B_0). The magnitude is in accord with calculations using approximate literature values of the susceptibility of water and 85% H_3PO_4 ($2\pi\Delta\chi = 0.63$ ppm). We expect our experimental value to be accurate within 0.05 ppm. Similarly, for CH_3CN solutions we calculate $\delta_{\mathrm{vert}} = \delta_{\mathrm{horiz}} + 1.82$ ppm. Related numbers for ^{51}V NMR shifts relative to those of $VOCl_3$ are $\delta_{\mathrm{vert}}(H_2O) = \delta_{\mathrm{horiz}}(H_2O) - 3.7$ ppm and $\delta_{\mathrm{vert}}(CH_3CN) = \delta_{\mathrm{horiz}}(CH_3CN) - 2.5$ ppm. Values of the diamagnetic susceptibility were obtained for the following compounds. (a) H_3PO_4, H_2O, CH_3CN: "Handbook of Chemistry and Physics"; CRC Press, Inc.: Boca Raton, FL, 1984. (b) $VOCl_3$: *J. Chim. Phys. Phys.-Chim. Biol.* **1970**, *67*, 1769–1772.

(13) (a) O'Donnell, S. E.; Pope, M. T. *J. Chem. Soc., Dalton Trns.* **1976**, 2290–2297. (b) Harmalker, S. P.; Leparulo, M. A.; Pope, M. T. *J. Am. Chem. Soc.* **1983**, *105*, 4286–4292.

(14) The electric field gradient q_{zz} and asymmetry parameter $\eta = (q_{yy} - q_{xx})/q_{zz}$ both contribute to the line width as does the molecular rotational correlation time τ_c. We expect τ_c(Keggin) < τ_c(Dawson) because of the smaller size and so attribute the similar line widths to larger q_{zz} and η values in Keggin compounds. Nevertheless, the crude features of the change in bonding upon vanadium substitution appear similar in the two families of compounds.

(15) The TBA salt was selected for the 2-D INADEQUATE experiment because of superior solubility. Note the chemical shift differences between the aqueous solution of the lithium salt (Figure 3) and acetonitrile solution of the TBA salt (Figure 4).

(16) The relative quantities of both species vary. Typically, 60–80% of the mixture is B-PW_9.

(17) In a representative reaction using heated PW_9, which is 60% B-PW_9 and 40% unknown (^{31}P MAS NMR), we observe the following distribution of products in the crude reaction mixtures. (a) With VO_2^+: 1,4,9-PV_3W_9 (59%), 1,4-PV_2W_{10} (6%), 1,2,3-PV_3W_9 23%, 1,2-PV_2W_{10} (7%), PVW_{11} (5%), traces of unidentified products; (b) With VO^{2+}: 1,4,9-PV_3W_9 (11%), 1,4-PV_2W_{10} (50%), 1,2,3-PV_3W_9 (8%), 1,2-PV_2W_{10} (7%), PVW_{11} (24%), traces of unidentified products. The approximate 60/40 ratio of (1,4,9 + 1,4)/1,2,3 + 1,2) suggests the identified species in thermolyzed $Na_9[PW_9O_{34}]$ is A-PW_9, or at least a precursor thereof.

0020-1669/86/1325-1239$01.50/0

reproduced in the text are captioned with specific details. IR spectra were recorded as mineral oil mulls using NaCl plates on a Perkin-Elmer 983 spectrometer. Elemental analyses were performed by Pascher Mikroanalytisches Laboratorium, Bonn, West Germany, or E&R Microanalytical Laboratory, Inc., Corona, NY. Water content in alkali-metal salts was determined by TGA from 25 to 400 °C.

Preparations. B-$Na_9[PW_9O_{34}]\cdot xH_2O$. $Na_2WO_4\cdot 2H_2O$ (120 g) was dissolved in 200 mL of water at room temperature, and the mixture was stirred 10 min (pH ~10.3). Dropwise, 2.75 mL of 85% H_3PO_4 was added, and the mixture was stirred a remaining 15 min (pH ~8.9). Slow addition of 35 mL of 12 M HCl to a final pH of 7.1 produces a white precipitate, which is collected after 4 h of stirring. During the first 20-mL addition of HCl a precipitate momentarily forms but goes back into solution. The final 15 mL of HCl produces a cloudy solution that develops further upon extended stirring. The precipitate is filtered and dried at room temperature, without washing. Yields are variable at 40–90 g of product.

Anal. Calcd (found) for 98.8% $Na_9[PW_9O_{34}]\cdot 7H_2O$ + 1.2% NaCl: Na, 8.44 (8.10); P, 1.20 (1.20); W, 63.8 (62.9); O, 25.3 (25.9); H, 0.54 (0.50); Cl, 0.71 (0.71); H_2O, 4.86 (4.80).

A duplicate preparation shows 0.7% NaCl. We have avoided washing because of degradation of the sample when observed by ^{31}P NMR.

Ten-gram quantities of this precursor anion were placed in $^1/_2$-in. test tubes that were placed in a heated block at 120 °C for 70–120 h. IR spectra and solid-state ^{31}P MAS NMR spectra show the desired[10a] conversion to B-$PW_9O_{34}^{9-}$.

1,4-$K_5[PV_2W_{10}O_{40}]$ and 1,4-$(TBA)_4H[PV_2W_{10}O_{40}]$. $VOSO_4\cdot 2H_2O$ (3.5 g) was stirred for 15 min in 100 mL of water (pH ~1.6). Slowly, 20-mg quantities of solid B-$Na_9[PW_9O_{34}]$ were added to the vigorously stirred solution, taking care that no white solid was visible in the ink-blue solution before the next addition. After 25 g of B-$Na_9[PW_9O_{34}]$ had been added, 1 mL of Br_2 was added to oxidize the mixture to a bright orange color. Solid KCl (12.5 g) was added to the solution, and the mixture was heated to 80 °C for 15 min. The solution was cooled to room temperature and filtered to give approximately 8 g of yellow $K_4[PVW_{11}O_{40}]$. The remaining filtrate was reduced in volume by ca. 50% by rotary evaporation and cooled in a 0 °C ice bath for 30 min to produce 15.5 g of the desired product. These crystals were recrystallized from a minimum of 80 °C pH 2 water cooled to 0 °C to give 7.0 g of product. IR and ^{51}V and ^{31}P NMR spectra indicated clean product, but we have been unable to obtain satisfactory elemental analyses for the potassium salt. Thus, the monoprotonated tetrabutylammonium salt was prepared by dissolving 2.5 g of the potassium salt in 40 mL of water and adjusting to pH 1 with 3 M HCl. A solution of 2 g of tetra-*n*-butylammonium bromide ((TBA)Br) in 50 mL of water was added. The orange powder was collected by vacuum filtration and washed with 3 × 100 mL of 60 °C water. The dried product was recrystallized from boiling acetonitrile to room temperature, collected, and washed with diethyl ether to yield 0.8 g of analytically pure product.

Anal. Calcd (found) for 1,4-$(TBA)_4H[PV_2W_{10}O_{40}]$: C, 21.5 (21.4); H, 4.08 (4.06); N, 1.56 (1.62); P, 0.86 (0.85); V, 2.84 (2.71); W, 51.3 (51.6); O, 17.9 (17.8); total, 100.00 (100.04).

IR and NMR analyses are given in the Results and Discussion. ^{183}W NMR were recorded by deprotonating the salt with 1 equiv of (TBA)OH/MeOH to increase the solubility. The isomeric purity of both 1,4-$(TBA)_5[PV_2W_{10}O_{40}]$ and 1,4-$(TBA)_4H[PV_2W_{10}O_{40}]$ are retained in refluxing CH_3CN for 100 h.

1,4,9-$K_6[PV_3W_9O_{40}]\cdot xH_2O$ and 1,4,9-$(TBA)_4H_2[PV_3W_9O_{40}]$. A 2.0-g sample of $NaVO_3$ was powdered and stirred with 100 mL of water for 15 min. Very slowly, 3 M HCl was added to reduce the pH from 8.1 to 0.8. While the HCl was being added, the characteristic orange color of $V_{10}O_{28}^{6-}$ formed and at lower pH was replaced by the pale yellow color of VO_2^+. Slow addition is necessary to inhibit V_2O_5 formation on the surface of undissolved $NaVO_3$. Trace amounts of V_2O_5 were removed by filtration. The 10–20 mg quantities of B-$Na_9[PW_9O_{34}]\cdot xH_2O$ were added slowly with stirring until a total of 15 g was added. The cherry red solution (pH ~1) was heated to 90 °C, 10 g of KCl was added, and the volume was reduced to 60 mL. Cooling of the solution to 40–60 °C produces yellow $K_4[PVW_{11}O_{40}]$, which is removed by filtration. The filtrate is cooled for 45 min in a 0 °C ice bath and filtered to give 9.1 g of orange powder. Overnight chilling yields a further 0.9 g of large red-orange crystals. Repeat preparations give similar overall yields of 10 g with some variation in the distribution of crops. A single recrystallization[18] of 7.2 g of crude product in water at pH 1.5 cooled from 80 °C to room temperature yields 4.9 g of acceptably pure $K_6[PV_3W_9O_{40}]\cdot 13H_2O$.

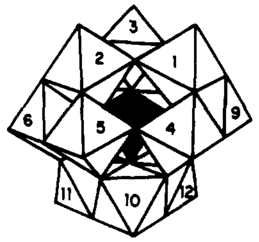

Figure 1. Numbering scheme for substituted Keggin ions.

Anal. Calcd (found) for $K_6[PV_3W_9O_{40}]\cdot 13H_2O$: K, 7.96 (7.66); P, 1.05 (1.08); V, 5.19 (5.48); W, 56.1 (57.0); O, 28.8 (28.2); H, 0.89 (0.65); H_2O, 7.9 (8.0); total, 100.0 (100.1). Presumably, the slightly low potassium value can be accounted for by partial protonation. Calcd (found) for $K_{5.7}H_{0.3}[PV_3W_9O_{40}]\cdot 13H_2O$: K, 7.59 (7.66); P, 1.06 (1.08); V, 5.21 (5.48); W, 56.4 (57.0); O, 28.9 (28.2); H, 0.89 (0.65); H_2O, 8.0 (8.0); total, 100.0 (100.1).

The doubly protonated TBA salt was made by dissolving 1 g of the potassium salt in 20 mL of water, adjusting the pH to 1 with 3 M HCl, and adding a solution of 1 g of (TBA)Br in 10 mL of water. The orange precipitate formed was washed with 150 mL of pH 1 water and dried to give 1.2 g of product. The compound was recrystallized from boiling acetonitrile cooled to 0 °C to give 0.43 g of analytical quality crystals.

Anal. Calcd (found) for $(TBA)_4H_2[PV_3W_9O_{40}]$: C, 22.28 (21.83); H, 4.27 (4.22); N, 1.62 (1.74); P, 0.90 (0.86); V, 4.35 (4.43); W, 47.9 (47.3); O, 18.6 (18.5); total, 100.0 (98.8).

IR and ^{51}V, ^{31}P, and ^{183}W NMR data are given in the Results and Discussion.

Results and Discussion

Compound Identification. The primary tool for identification of 1,4-$PV_2W_{10}O_{40}^{5-}$ and 1,4,9-$PV_3W_9O_{40}^{6-}$ (Figure 1) is 1- and 2-D ^{183}W NMR combined with ^{51}V decoupling. Once the structures are established, ^{51}V and ^{31}P NMR provide rapid identification because of their inherently higher sensitivity.

(i) ^{31}P and ^{51}V NMR and IR Spectra. ^{31}P NMR chemical shifts of phosphovanadotungstates are restricted to a limited chemical shift range, so accurate referencing of spectra is necessary to allow meaningful comparisons among different laboratories. The major problem is the diamagnetic susceptibility difference of the usual 85% H_3PO_4 reference and water solvent, producing a 0.70 ppm difference between spectra of aqueous solutions recorded with a superconducting-magnet geometry[12] (vertical B_0 field) and an electromagnet or permanent magnet with a horizontal B_0 field. Precise temperature control is also required, and pH must be controlled. Table I lists our data for 30 °C spectra obtained with a superconducting magnet by using the sample replacement method to externally reference to 85% H_3PO_4. We find no significant difference between these data and those with an additional concentric H_3PO_4 capillary contained within the D_2O lock capillary. Data are given for $K_3[PW_{12}O_{40}]$ and $K_4[PVW_{11}O_{40}]$ as well as both pairs of $K_5[PV_2W_{10}O_{40}]$ and $K_6[PV_3W_9O_{40}]$ isomers and TBA salts. There is a general downfield shift with increasing vanadium substitution, and B-type compounds are further downfield than their A-type counterparts. Deprotonation of TBA salts of A-type species produces a downfield shift while the corresponding B-type compounds move upfield.

^{51}V NMR chemical shifts are strongly pH-dependent in the di- and trivanado-substituted compounds. Susceptibility differences are less of a problem[12] since lines are broader and chemical shift ranges are larger. Line width is an important parameter[13] and is included with chemical shift data in Table I. No clear trends in chemical shift are evident, but several other features are noteworthy. Line widths increase in the order $V_1 < V_2 < V_3$, but B-type species, with edge sharing of vanadium octahedra, are significantly sharper than their A-type analogues. There is a striking parallel between these line widths (PV, 25 Hz; 1,4-PV_2, 70 Hz; 1,4,9-PV_3, 100 Hz) and those of the corresponding Dawson compounds[13b] (α_2-P_2VW_{17}, 33 Hz; α-$P_2V_2W_{16}$, 70 Hz; α-$P_2V_3W_{15}$, 130 Hz), indicating similar bonding characteristics.[14] Higher pH causes a substantial downfield shift and line narrowing in the trisubstituted species presumably because of deprotonation. In 1,2,3-$(TBA)_4H_2[PV_3W_9O_{40}]$ at 30 °C proton mobility is suffi-

---

(18) Superior results are obtained with a MeOH-saturated, aqueous, pH 1 crystallization from 80 to 0 °C: Finke, R. G.; Rapko, B.; Rolly, L. J., personal communication.

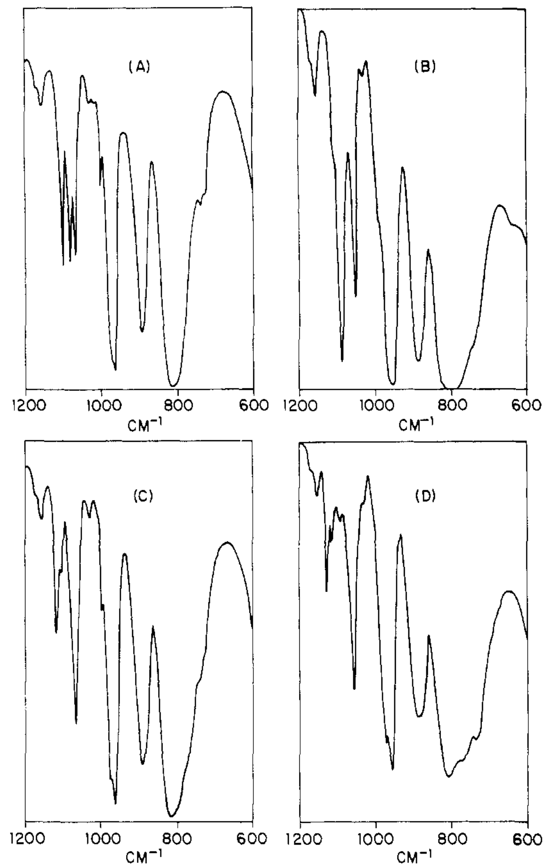

Figure 2. IR spectra (mineral oil mulls) of tetra-*n*-butylammonium (TBA) salts of specific di- and trivanado-substituted phosphotungstates: (A) 1,2-$(TBA)_4H[PV_2W_{10}O_{40}]$; (B) 1,2,3-$(TBA)_4H_2[PV_3W_9O_{40}]$; (C) 1,4-$(TBA)_4H[PV_2W_{10}O_{40}]$; (D) 1,4,9-$(TBA)_4H_2[PV_3W_9O_{40}]$.

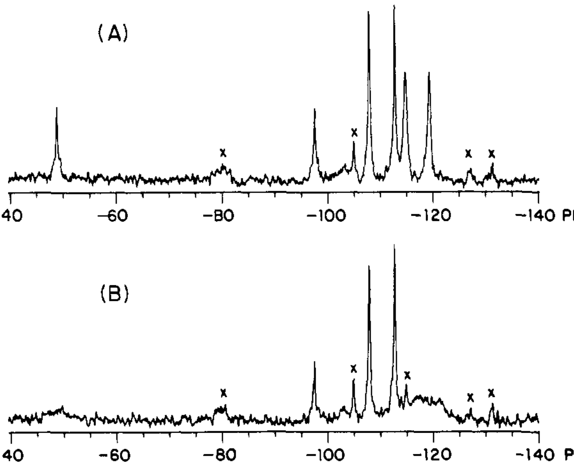

Figure 3. ^{183}W NMR spectra of 1,4-$Li_5[PV_2W_{10}O_{40}]$ (A) with and (B) without ^{51}V decoupling (samples approximately 0.1 M in D_2O; 30 °C; 8192 shots in 2.3 h). Impurity lines (×) are due to the 1,2-$Li_5[PV_2W_{10}O_{40}]$ isomer.

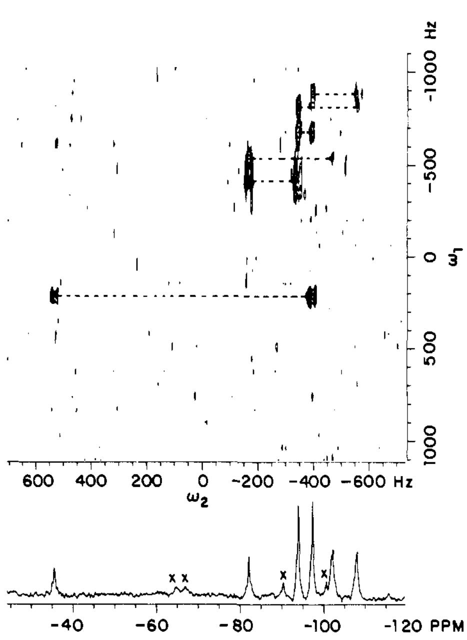

Figure 4. 2-D ^{183}W INADEQUATE connectivity pattern of 0.13 M 1,4-$(TBA)_5[PV_2W_{10}O_{40}]$ in CD_3CN/DMF at 30 °C (10240 shots in each of 32 × 2K files; total time 90 h).

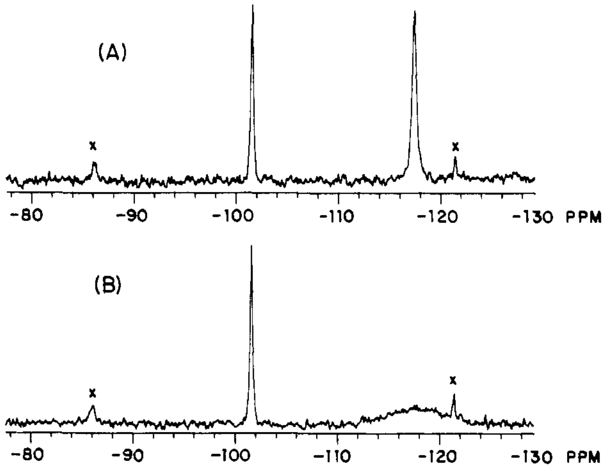

Figure 5. ^{183}W NMR spectra of approximately 0.1 M 1,4,9-$K_6[PV_3W_9O_{40}]$ in D_2O at 30 °C and pH 2 (A) with and (B) without ^{51}V decoupling (1024 shots in 35 min). Impurity lines are due to 1,2,3-$K_6[PV_3W_9O_{40}]$.

ciently limited that two separate ^{51}V resonances are observed. At increased temperatures these sites exchange as proton mobility increases. Similar observations, without exchange, are also reported[4] for $HSiV_3W_9O_{40}{}^{6-}$.

IR spectra in the 600–1200-cm^{-1} range are shown in Figure 2 for the different PV_2W_{10} and PV_3W_9 isomers, and the dominant band positions are also listed in Table I. The above combination of IR and ^{31}P and ^{51}V NMR characterization should allow other workers to identify these species.

(ii) ^{183}W NMR of 1,4-$PV_2W_{10}O_{40}{}^{5-}$. Figure 3 shows the ^{183}W NMR spectrum of a sample of 1,4-$Li_5[PV_2W_{10}O_{40}]$ in D_2O in the absence and presence of ^{51}V decoupling. In the decoupled spectrum, the major lines (−48.8, −97.5, −107.9, −112.7, −114.7, −119.3 ppm) integrate 1:1:2:2:2:2 with minor impurity lines of 1,2-$PV_2W_{10}O_{40}{}^{5-}$ evident. Of the five positional isomers of the disubstituted Keggin structure only the 1,2- and 1,4-isomers have this intensity distribution. Since the 1,2-compound has been identified,[1] and 1,4-isomer could be assigned by difference. However, for rigor, the ^{51}V-coupled spectrum and the 2-D ^{183}W connectivity pattern were also measured.

In the absence of ^{51}V decoupling one of the lines of intensity 1 (−49 ppm) broadens substantially, more than can be accounted for[1] on the basis of coupling to a single ^{51}V and consistent with edge sharing of the tungsten with two equivalent vanadium atoms. Similarly, two lines of intensity 2 broaden because of their proximity and corner coupling to vanadium. Both of these observations are in accord with the formulation as the 1,4-isomer.

Figure 4 shows the ^{183}W–O–^{183}W connectivity pattern obtained from a 2-D INADEQUATE experiment on 1,4-$(TBA)_5[PV_2W_{10}O_{40}]$ in acetonitrile-d_3.[15] On the basis of earlier established arguments,[1] the observed connections W_9–$W_8(W_{12})$ (corner), W_6–$W_7(W_{11})$ (corner), W_6–$W_2(W_5)$ (edge), $W_7(W_{11})$–$W_8(W_{12})$ (edge), $W_7(W_{11})$–$W_3(W_{10})$ (edge), and $W_8(W_{12})$–$W_3(W_{10})$ (edge) are only compatible with the 1,4-isomer with the assignment of peaks W_9 (−35.7 ppm), W_6 (−82.2 ppm), $W_7(W_{11})$

Table I. ^{31}P and ^{51}V NMR[a] and IR Characterization Data of Polyoxoanions

compd	pH	$\delta(^{31}P)$[b]	$\delta(^{51}V)$ (line width, Hz)	ν, cm^{-1}
$K_3[PW_{12}O_{40}]$		−14.55		1081 (s), 985 (s), 892 (s), 818 (vs)
$K_4[PVW_{11}O_{40}]$		−14.19	−557.3 (25)	1101 (m), 1077 (s), 1065 (sh), 982 (s), 881 (s)
1,2-$K_5[PV_2W_{10}O_{40}]$	2.0	−13.61	−548.6 (120)	
1,2-$(TBA)_5[PV_2W_{10}O_{40}]$		−13.17	−539.0 (215)	
1,2-$(TBA)_4H[PV_2W_{10}O_{40}]$		−13.51	−560.9 (270)	1098 (m), 1078 (m), 1062 (m), 961 (s), 891 (s), 814 (vs)
1,4-$K_5[PV_2W_{10}O_{40}]$	2.0	−13.46	−528.4 (70)	
1,4-$(TBA)_5[PV_2W_{10}O_{40}]$		−12.95	−515.7 (305)	
1,4-$(TBA)_4H[PV_2W_{10}O_{40}]$		−12.20 (br)	−561.4 (375)	1112 (m), 1062 (s), 959 (s), 888 (s), 812 (vs)
1,2,3-$K_6[PV_3W_9O_{40}]$	1.8	−13.41	−566.1 (275)	
	5.0	−12.82	−533.1 (225)	
1,2,3-$(TBA)_6[PV_3W_9O_{40}]$		−12.53	−523.6 (520)	
1,2,3-$(TBA)_4H_2[PV_3W_9O_{40}]$		−13.09 (br)	−555.8, (180) 1 V	1087 (s), 1052 (m), 952 (s), 885 (s), 805 (vs)
			−568.8, (700) 2 V	
1,4,9-$K_6[PV_3W_9O_{40}]$	2.0	−11.38	−530.6 (100)	
	5.5	−12.16	−499.4 (70)	
1,4,9-$TBA_6[PV_3W_9O_{40}]$		−11.68	−484.9 (170)	
1,4,9-$TBA_4H_2[PV_3W_9O_{40}]$		−9.68	−540 to −570, broad overlapped	1124 (m), 1053 (m), 953 (s), 879 (s), 802 (vs)

[a] NMR spectra are recorded in a vertical B_0 field geometry at 30 °C with a concentric D_2O capillary for field/frequency lock. Alkali-metal salts are in aqueous solution while TBA salts are in acetonitrile. [b] See ref 12.

(−94.0 ppm), $W_8(W_{12})$ (−97.4 ppm), $W_2(W_5)$ (−107.2 ppm), $W_3(W_{10})$ (−108.1 ppm). Values in parentheses indicate symmetry equivalence. The only connectivity not observed is $W_2(W_5)$–$W_3(W_{10})$ (corner), because both peaks are broadened due to incomplete ^{51}V decoupling.

(iii) ^{183}W NMR of 1,4,9-$PV_3W_9O_{40}{}^{6-}$. Figure 5 shows a conventional 1-D ^{183}W NMR spectrum of $K_6[PV_3W_9O_{40}]$ with and without ^{51}V decoupling. The decoupled spectrum integrates (−101.6 ppm, 3 W; −117.4 ppm, 6 W) with the coupled spectrum showing serious broadening of the upfield line. We are unable to measure the ^{183}W–O–^{183}W satellite lines but can set an upper limit of $J < 10$ Hz. All these observations are only consistent with a 1,4,9-$PV_3W_9O_{40}{}^{6-}$ isomer on the basis of principles outlined previously.[1]

Syntheses. Both vanadium(IV) and vanadium(V) readily react with $PW_9O_{34}{}^{9-}$ to give $PV_nW_{12-n}O_{40}{}^{(n+3)-}$ (n = 1, 2, 3). The important requirements necessary for successful isolation of both 1,4-$PV_2W_{10}O_{40}{}^{5-}$ and 1,4,9-$PV_3W_9O_{40}{}^{6-}$ are as follows: (i) the use of heated $Na_9[PW_9O_{34}]$ as a precursor; (ii) the order of addition of reactants; (iii) the preferential formation of V_2 species when vanadium(IV) is used as reactant and V_3 species when vanadium(V) is utilized; (iv) solubility differences (as potassium salts) between different isomers and different species.

In spite of its widespread use as a precursor polyanion, $PW_9O_{34}{}^{9-}$ is poorly characterized by elemental analysis. Our attempts to provide a starting material that is better defined have been only partially successful. Our synthesis uses HCl as the condensing acid rather than HOAc described in the original literature report because the latter acid is clearly evident in the final product both through its odor and through IR analysis. Chloride is evident in our sample, and recrystallization is not successful because of anion degradation. Nevertheless, elemental analyses are adequate. Solid-state ^{31}P MAS spectra clearly show only one phosphotungstate species. Heated $Na_9[PW_9O_{34}]$ shows a major new species that we attribute to B-PW_9 and an unidentified impurity compound.[10a,16]

When heated $Na_9[PW_9O_{34}]$ is dissolved in water, it quickly reverts to A-PW_9, in addition to other species. Therefore, our synthetic procedures adopt the slow addition of B-PW_9 *solid* to preformed solutions of the vanadium reactant (either $VOSO_4$ or $VO_2{}^+$). In this manner the response represents a competition between reaction of B-PW_9 with vanadium or conversion to other phosphotungstates prior to reaction. Unfortunately, because our B-PW_9 contains the unidentified phosphotungstate, it is difficult to quantify the specificity of the conversion of B-PW_9 to 1,4-PV_2 and 1,4,9-PV_3. Nevertheless, there are major preferences for the B-type compounds.[17] We have varied the thermolysis conditions for the A- → B-PW_9 conversion and find 120 °C gives optimum yield of B-type products by approximately 2/1 in crude reaction mixtures. Simple recrystallization then affords pure compounds. It is worth noting that any PW_9 species requires an additional 1 equiv of tungstate to produce divanado-substituted species. Given the multitude of known phosphotungstates,[8,9] it is not surprising we cannot identify the source.

Reaction of B-PW_9 with $VO_2{}^+$ favors PV_3 production over PV_2 formation by about (5–10)/1 whereas the opposite distribution is observed in reactions with VO^{2+} and subsequent oxidation with Br_2. Presumably, pH control could also be used to achieve the same result, but we have not pursued this option because of the ease of our procedure.

With isomer control via the PW_9 precursor and degree of substitution regulated by the vanadium oxidation state, the final governor of purity is the different solubilities of species in the mixtures. $K_4[PVW_{11}O_{40}]$ is by far the least soluble of all species present and is easily removed by an initial filtration. Also, the A-type isomers are more soluble than their B-type counterparts, allowing their separation. Finally, 1,4,9-PV_3 is less soluble than 1,4-PV_2, allowing selective crystallization.[18]

Acknowledgment. It is a pleasure to acknowledge R. G. Finke and B. Rapko (University of Oregon) for fruitful discussions of supported organometallics and mixed-solvent crystallization.